Covid-19 and mobility: determinant or consequence?

Hippolyte d'Albis, Emmanuelle Augeraud-Véron, Dramane Coulibaly, Rodolphe Desbordes

PARIS SCHOOL OF ECONOMICS
ECOLE D'ECONOMIE DE PARIS

WORKING PAPER N° 2023 – 20

COVID-19 and Mobility: Determinant or Consequence?

Hippolyte d'Albis
Emmanuelle Augeraud-Veron
Dramane Coulibaly
Rodolphe Desbordes

JEL Codes: I1; C61; C32.
Keywords: COVID-19; Epidemic Models; Mobility.

anr agence nationale de la recherche
AU SERVICE DE LA SCIENCE
INVESTIR L'AVENIR

COVID-19 and Mobility: Determinant or Consequence?*

Hippolyte d'Albis[†], Emmanuelle Augeraud-Véron[‡]

Dramane Coulibaly[§], Rodolphe Desbordes[¶]

Abstract

This paper disentangles the relationship between COVID-19 propagation and mobility. In a theoretical model allowing mobility to be endogenously determined by the COVID-19 prevalence rate, we show that an exogenous epidemic shock has an immediate effect on mobility whereas an exogenous mobility shock influences epidemic variables with a delay. In the long run, exogenous disease contagiousness and mobility jointly shape epidemiological outcomes. The short-run theoretical result allows us to recover, empirically, the causal impacts of mobility and COVID-19 hospitalisations on each other in France. We find that hospitalisations are highly sensitive to mobility whereas mobility is little influenced by hospitalisations. In France, it seems therefore that voluntary social distancing would not have been effective to control the epidemic, in the absence of social distancing mandates.

Keywords: COVID-19; Epidemic Models; Mobility.

J.E.L. codes: I1; C61; C32.

*The authors thank the special editor of this issue and two referee for constructive comments and critics and Sarah Chauveau for excellent research assistance. This analysis uses data provided by Facebook, under the Data For Good initiative. None of the authors have contractual relationships with Facebook.

[†]Paris School of Economics

[‡]BSE-Bordeaux Sciences Economiques

[§]Université Lumière Lyon 2, GATE

[¶]Corresponding author. SKEMA Business School-Université Côte d'Azur, Campus Grand Paris, 5 quai Marcel Dassault, Suresnes, 92150, France. Telephone number: +33 171 133 900. E-mail: rodolphe.desbordes@skema.edu.

1 Introduction

The COVID-19 pandemic has claimed, so far, an excess of 5 millions lives worldwide and generated a 7% loss in 2020 global output relative to pre-pandemic forecast (Levy Yeyati and Filippi, 2021).[1] These two numbers are often interpreted in the context of a health-economy trade-off (Fernández-Villaverde and Jones, 2020). Governments, in an attempt to slow down the spread of the epidemic, avoid exceeding health care capacity ('flattening the epidemic curve'), and gain time until the development of a successful vaccine, have implemented drastic social distancing measures such as full lock-downs (stay-at-home policies). The price to pay has been a large fall in national income and individual earnings since, in most cases, workers and consumers could not move, produce, and purchase (Eichenbaum et al., 2021). In addition, treatment of other diseases was neglected, school closures led to delays in human capital accumulation, and some psychological disorders increased (Escandón et al., 2021; Joffe, 2021).

It is still debated whether these human and economic costs could have been avoided. As emphasised by the rational epidemics literature (Philipson, 2000), voluntarily social distancing could be a natural behavioural response to a rise in the infection rate. In this case, the most risk-averse or susceptible population would take, on their own, the necessary non-pharmaceutical measures to reduce the probability of being infected, and possibly infecting others, with potentially fewer negative economic and social impacts. It would then be unclear whether reducing mobility further by legally forcing most people to stay at home would provide additional health benefits.

The COVID-19 experience provides credence to rational epidemics theory. There is a large empirical literature, showing that the share of the overall mobility response attributed to voluntarily social distancing can be very large.[2] For example, the IMF (Caselli et al., 2021) reports a 60% share in advanced economies while Goolsbee and Syverson (2021) estimate this share to be as high as 88% in the United States. Nevertheless, generalisations ought to be avoided. Milani (2021) highlights that the response of mobility to the growth rate in COVID-19 was highly heterogeneous across countries in early 2020: strongly negative in France (where a lockdown was imposed) and null in Sweden (with a more permissive approach than France).

[1] For COVID-19 statistics, see `https://ourworldindata.org/coronavirus-data`.

[2] Good surveys of the literature can be found in Allen (2021), Bricongne and Meunier (2021), Brodeur et al. (2021), and Chernozhukov et al. (2021).

The heterogeneity of these estimates indicates that voluntary social distancing may be context-specific, implying that governments across countries may not necessarily be able to rely on voluntary changes in behaviours to control an epidemic.

In this paper, we contribute to the debate on the determinants of epidemic-related mobility in two ways. We first develop a theoretical epidemiological framework in which the spread of the epidemic rises with mobility, which can be constrained by the government but is also expected to react negatively to the rise in the infection rate. More specifically, we consider a compartmental epidemiological model that features the dynamics of SARS-Cov-2 and extends previous works of Arino et al. (2006), (Augeraud-Véron, 2020), Liu et al. (2020a), Liu et al. (2020b), Aubert and Augeraud-Véron (2021), and d'Albis and Augeraud-Véron (2021) and complement recent researches that introduce mobility in economic-epidemic models (such as La Torre et al. (2022), Makris (2021), Goenka et al. (2022), Hritonenko and Yatsenko (2022) and Fabbri et al. (2023)). Our model allows us to disentangle the short-run and long-run interactions between mobility and the infection/death rates. In the short run, a mobility shock has no immediate impact on the epidemic variables whereas a shock to the infection rate has an immediate effect on mobility. In the long run, the numbers of infected people and deceased depend on the two exogenous parameters governing, respectively, disease contagiousness and mobility.

Afterwards, we test the implications of our model, exploiting finely-grained French data on mobility and hospitalisation cases within departments over the period of March 2020-February 2021. Thanks to the panel and sub-national structure of our data, we can control for common time fixed effects (e.g. nationally-imposed lockdown, mandatory face protection, compulsory days of teleworking), department-specific fixed effects (e.g. composition of the population which can influence the share of essential workers), and department-specific time trends (e.g. the epidemic may be at different stages of development). Given that all substantial non-pharmaceutical interventions were decided at the national level and we include time fixed effects, we specifically identify the voluntary behavioural response of the local population to local health shocks.[3] As highlighted above, this is a key issue in the empirical literature on the

[3]Local health shocks may be particularly relevant in guiding individuals' decisions because informational and emotional proximity to the local spread of an epidemic is likely to be facilitated by geographically-concentred

determinants of population mobility during the Covid-19 epidemic.

We adopt a vector autoregressive regression (VAR) approach to carry our estimations relating mobility to hospitalisations and vice-versa. Under the restriction suggested by our theoretical model that exogenous changes in mobility do not immediately influence the epidemic variables, this methodology allows us to recover the dynamic causal effects of exogenous shocks to mobility and hospitalisations. Figure 1 highlights that there is nothing straightforward about the identification of these effects since it suggests that higher mobility is associated with lower hospitalisations, which is at odd with basic epidemiological intuitions and suggests a significant causal direction from health indicator to mobility.

Figure 1: Weekly national mobility and weekly hospitalisations

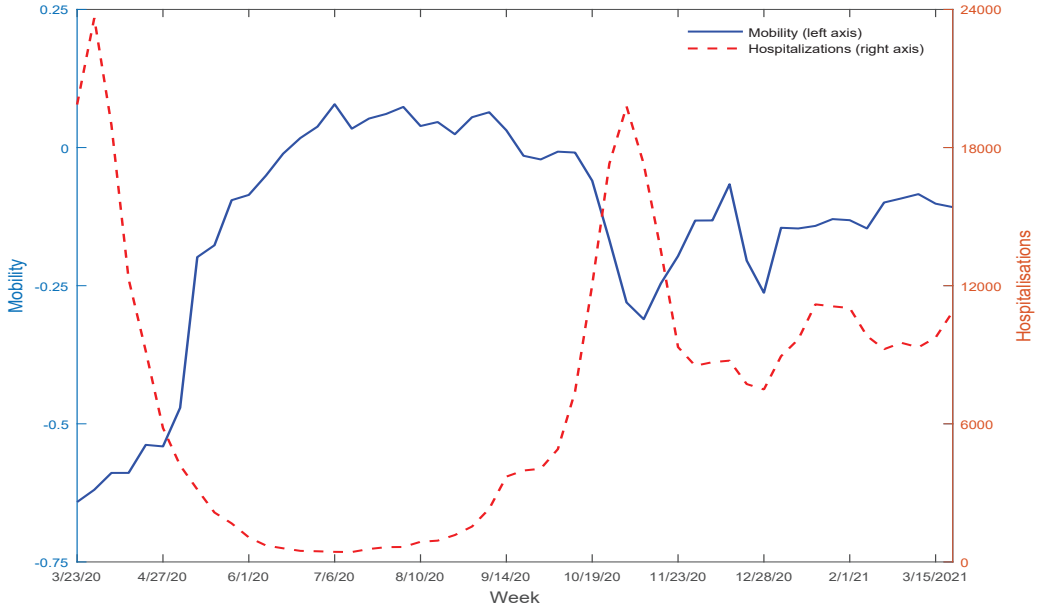

In line with our theoretical model, we empirically find that positive exogenous mobility shocks are associated with a substantial increase in the number of hospitalisations. We also find that positive exogenous hospitalisation shocks are associated with a fall in mobility. However, this effect, although statistically significant, is extremely small. Since our empirical set-up isolates a voluntary behaviour effect, this last result suggests that, in France, in the absence of social distancing mandates, voluntary social distancing would not have meaningfully occurred

social networks. Tangentially, our ability to detect the effects of mobility shocks on hospitalisations indicate that a national lockdown had heterogeneous consequences at the departmental level.

and therefore the spread of the epidemic, with its associated negative health consequences, would have been much higher. Said differently, the changes in mobility illustrated in Figure 1 are likely to have been mostly driven by mandatory mobility restriction policies.

Our paper is related to three distinct, but inter-related literature. First, our explicit modelling of mobility can be understood as an extension of meta population models, which incorporate movement models into standard epidemiological models (see Citron et al. (2021) for a review). Second, as mentioned previously, there is an on-going fierce debate about the retrospective effectiveness of lockdown measures. We find direct and robust evidence that, in the case of France, voluntary distancing behaviour cannot explain mobility reductions. Tangentially, our ability to detect the effects of mobility shocks on hospitalisations indicate that a national lockdown had heterogeneous consequences at the departmental level. Our results corroborate and extend those of Pullano et al. (2020). In an observational study of one week in April 2020, they find an absence of mobility changes in France before the lockdown, strong but heterogeneous mobility reductions during the lockdown, and a positive correlation between mobility reductions and the lagged cumulative number of hospitalisations per inhabitants. Note that Galeazzi et al. (2021) also report a strong impact of the lockdown on national mobility in France, four to five times larger than in Italy or the United Kingdom. Lastly, our paper confirms that the contribution of lockdowns to mobility reduction is heterogeneous across countries. Said differently, the external validity of the U.S. findings for the rest of the world is doubtful because behavioural outcomes appear to be context-specific.

2 An Epidemiological Model with Mobility

Our theoretical framework is an epidemiological model with two infectiousness compartments. Some infected individuals may present no or mild symptoms and thus contribute unknowingly to the propagation of the virus, whereas others may present so severe symptoms that they need to be hospitalized. A time $t \in \mathbb{R}^+$, the total population is denoted $P(t)$ and satisfies:

$$P(t) = S(t) + A(t) + H(t) + R(t), \tag{1}$$

where $S(t)$ denotes the susceptible individuals, who are healthy and can be contaminated, $A(t)$ the contaminated individuals without symptoms, $H(t)$ the contaminated individuals with symptoms who are hospitalized, and $R(t)$ the individuals who recovered and are fully immunized. Contamination is thus due to asymptomatic infectious individuals and, at each date t, a proportion $\tau(m(t))A(t)$ of the susceptible become infected. A specificity of our analysis is that the transmission rate, $\tau(.)$, positively depends on a mobility index, $m(t) \in [0,1]$, whose dynamics are described below. Newly contaminated individuals are first asymptomatic and may became symptomatic at rate $\nu > 0$ or may recover at rate $\eta_1 > 0$. Hospitalized individuals either die, at rate $\gamma > 0$, or recover, at rate $\eta_2 > 0$. The dynamics of the compartments are given by the following system:

$$S'(t) = -\tau(m(t))S(t)A(t), \tag{2}$$

$$A'(t) = \tau(m(t))S(t)A(t) - \nu A(t) - \eta_1 A(t) \tag{3}$$

$$H'(t) = \nu A(t) - (\eta_2 + \gamma)H(t), \tag{4}$$

$$R'(t) = \eta_2 H(t) + \eta_1 A(t), \tag{5}$$

where the notation x' stands for $dx(t)/dt$. The initial conditions satisfy: $S(0) = S_0 > 0$, $H(0) = H_0 > 0$, $A(0) = A_0 > 0$ and $R(0) = 0$. The latter initial condition suggests that the epidemics is just starting at $t = 0$. We thus have: $P_0 = S_0 + H_0 + A_0$. Moreover, using system (2)-(5), we deduce from (1) that:

$$P'(t) = -\gamma H(t). \tag{6}$$

Thus, in the absence of the epidemics, the population is constant (with no births, deaths, nor migration) and supposed to be equal to 1.

The dynamics of the mobility index $m(t)$ are supposed to decrease with the inflow of newly hospitalized, $\nu A(t)$, and with its own level. We have:

$$m'(t) = a(1 - k_1 - k_2 \nu A(t) - m(t)) \text{ if } m(t) > 0, \tag{7}$$

with $m(0) = m_0$, $a > 0$, $k_1 \in (0,1)$ and $k_2 \in (0, 1-k_1)$. Parameter k_1 influences the level

of mobility and, most importantly, when there is no disease (i.e. for $A(t) = 0$) we see that the mobility index $m(t)$ converges to a steady-state normalized to $\overline{m} = 1 - k_1$. Hence, the larger k_1, the lower the mobility. Below, we use this parameter to characterize exogenous shocks to mobility by considering temporary change in the level of k_1. Importantly, those shocks are considered as exogenous because they do not depend on the state of the epidemics. Parameter k_2 represent the reaction of individual's mobility to the number of newly hospitalized individuals. This reflect both the perception of individuals that may want to reduce their risk exposure and the response of the Government that may react by enforcing various public policies, such as lockdown or school closures. Finally, we assume that a is large compared to all the other parameters of the model, and thus we write a as $a = \lambda/\varepsilon$, with $\lambda > 0$ and $0 < \varepsilon \ll 1$. Thus, the equation (7) can be rewritten as follows:

$$\varepsilon m'(t) = \lambda \left(1 - k_1 - k_2 \nu A(t) - m(t)\right). \tag{8}$$

As mentioned above, a key assumption of the model is that the contact rate $\tau(.)$ increases with mobility. We assume the following relation between those two variables:

$$\tau(m(t)) = \xi \frac{m(t)}{c + m(t)}, \tag{9}$$

where $\xi > 0$ is a scaling parameter that captures the infectivity capacity of the pathogen and where $c > 0$ is to be used to represent an exogenous shock in the epidemics. When c decreases temporarily, the contact rate (for a given mobility) increases, which translates into an increase in the number of infectious persons.

Below, we first consider the general properties of the model without shocks on parameters. Then, we analyze the impact an exogenous mobility shock, represented by a temporary reduction in k_1, and a exogenous shock on the epidemic force represented by a temporary increase in c. These responses are then compared with our empirical estimates.

Let us first consider the steady-state of our model.

Lemma 1. *There exists a unique steady state that satisfies:* $\lim_{t\to+\infty} P(t) = \lim_{t\to+\infty} S(t) = S_\infty > 0$, $\lim_{t\to+\infty} A(t) = \lim_{t\to+\infty} H(t) = \lim_{t\to+\infty} R(t) = 0$ *and* $\lim_{t\to\infty} m(t) = 1 - k_1$.

Proof. See the Appendix. □

This steady-state is a Disease Free Equilibrium, as the epidemics has disappeared. The reproduction number is computed around this steady-state.

Lemma 2. *The reproduction number of system (2)-(5) is*:

$$R_0 = \frac{\xi}{\left(1 + \frac{c}{(1-k_1)}\right)(\eta_2 + \gamma)}. \tag{10}$$

Proof. See the Appendix. □

Given our parameter restrictions, the reproduction number is positive and we can see that it decreases with k_1, the exogenous mobility parameter. Hence, the reproduction number increase when the mobility exogenously increases. Let ε_{k_1} be the elasticity of the reproduction number with respect to k_1, we obtain:

$$\varepsilon_{k_1} = \frac{-ck_1}{(1 + c - k_1)(1 - k_1)} < 0. \tag{11}$$

Similarly, the reproduction number decreases with c, which implies that it increases with an exogenous shock on the epidemics.

We now show that the dynamic system of our model, named $\mathcal{P}$ and given by equations (2)-(5) and (8), is a two-time scale model with slow time t and fast time z, defined as $t = \varepsilon z$.

Lemma 3. *Given the initial condition* $(S_0, A_0, H_0, 0, m_0)$*, the solution of system* $\mathcal{P}$ *quickly converges to the neighborhood of the slow manifold, whose equation is given by:*

$$L = \{(S, H, A, R, m), m = 1 - k_1 - k_2\nu A\}, \tag{12}$$

where the slow motion takes place. The slow motion is the solution of system $\mathcal{Q}$*, defined as*

follows:

$$S'(t) = -\tau(1-k_1-k_2\nu A(t))S(t)A(t), \tag{13}$$

$$A'(t) = \tau(1-k_1-k_2\nu A(t))S(t)A(t)-\nu A(t)-\eta_1 A(t), \tag{14}$$

$$H'(t) = \nu A(t)-(\eta_2+\gamma)H(t), \tag{15}$$

$$R'(t) = \eta_2 H(t)+\eta_1 A(t). \tag{16}$$

Proof. See the Appendix. □

A key property of our model is that the mobility index quickly converges. On the slow motion, one has $m'(t)=0$ and $m(t)=1-k_1-k_2\nu A(t)$. Let us turn to the analysis of system Q. We first consider a change in variable and introduce the inflow of new hospitalizations, which is a key variable of the empirical analysis. It is now denoted H_{osp} and satisfies $H_{osp}(t)=\nu A(t)$. Note that $H_{osp}(t)$ is distinct from $H(t)$, which represents the stock of hospitalized individuals. Equations (13) and (14) enable to obtain the path (S,H_{osp}) by solving:

$$\frac{dH_{osp}}{dS} = -\nu+\frac{(\nu+\eta_1)\nu}{\tau(1-k_1-k_2H_{osp})S}. \tag{17}$$

We then obtain:

Lemma 4. *The path (S,H_{osp}) is concave. Moreover, H_{osp} decreases as S decreases if:*

$$S<\frac{(\nu+\eta_1)}{\xi}\left(\frac{c}{1-k_1-k_2H_{osp}}+1\right), \tag{18}$$

while H_{osp} increases as S decreases otherwise.

Proof. See the Appendix. □

Lemma 4 permits do draw the phase diagram of our system. Figure 2 provides an example for a temporary increase in mobility. The blue curve is defined as the locus (S,H_{osp}) such that $dH_{osp}/dS=0$. On the right (resp. left) hand side of this curve H_{osp} is increasing (resp. decreasing). The green curve is the locus (S,H_{osp}) that solve equation (32) for a given k_1,

namely $k_1 = 0.8$. As all parameters are constant[4], we call it the "no-shock curve". On the contrary, the red curve is obtained with a parameter k_1 which is not constant across time as we assume that $k_1 = 0.8$ for $t \in [0, 50] \setminus [1, 2]$ and $k_1 = 0.7$ for $t \in [1, 2]$. To visualize the effect of the shock, we use a plain line for $t \in [0, 1]$, a dash-dotted line for $t \in [1, 2]$ and a dashed line for $t \in [2, 50]$.

Figure 2: Phase plane $(S(t), H_{osp}(t))$ for counterfactual and shocked trajectories

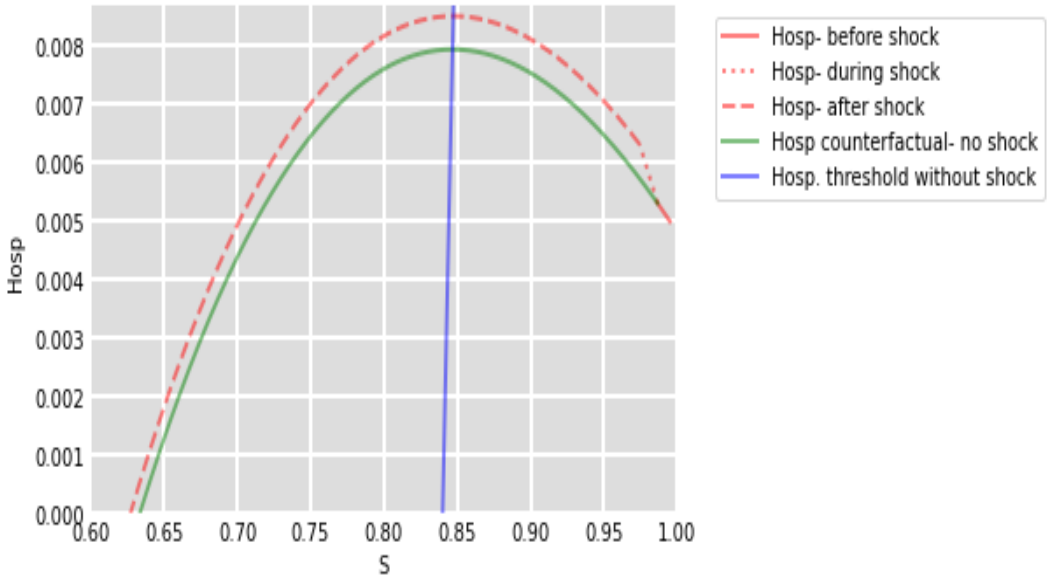

It is useful to define the "epidemic peak" as the maximal value H_{osp} can reach for a given set of parameters and initial conditions. It is obtained as the solution of $dH_{osp}/dS = 0$. There exists an epidemic peak if the initial conditions and parameters are such that $dH_{osp}/dS > 0$, i.e. if condition (18) is initially satisfied. From (18), we may immediately conclude the following:

Corollary. *For a given set of parameters and initial conditions, there exists a unique epidemic peak if* $c > c^*$*, where:*

$$c^* = \left(\frac{\xi}{(\nu + \eta_1)} S_0 - 1 \right) (1 - k_1 - k_2 \nu A_0) . \tag{19}$$

[4]Parameters are: $\eta_1 = \eta_2 = 0.1, \gamma = 0.2, k_2 = 0.3, c = 0.4, \xi = 1.25, \nu = 0.25, A(0) = 0,02, S(0) = 0,98$.

Similarly, one may define k_1^* such that there exists a unique epidemic peak if $k_1 > k_1^*$.

We now turn to study the consequence of a temporary shock on k_1 and c on the inflow of new hospitalizations and on mobility. We compare a trajectory affected by a given shock to the counterfactual trajectory, which is defined as the one without shock.

Lemma 5. *An exogenous increase of mobility immediately increases the inflow of new hospitalizations H_{osp}, compared to the counterfactual case. The difference between the flow associated with the shocked trajectory and that of the counterfactual increases throughout the interval during which the shock occurs.*

Proof. See the Appendix. □

The proof of this Lemma relies on that facts that dH_{osp}/dS increase with k_1 and that $dS < 0$. The lemma is illustrated with simulations using the same parameters as above. Figure 3 gives the evolution of the flow of newly hospitalized $H_{osp}(t)$. We see that the slope of the dash dotted red line is larger than that of the green line.

Figure 3: Inflow of new hospitalizations ($H_{osp}(t)$) along the shocked trajectory ($k_1 = 0.8$ for all $t \in [0, 50] \setminus [1, 2]$ and $k_1 = 0.7$ for $t \in [1, 2]$) and the counterfactual case ($k_1 = 0.8$ for all $t \in [0, 50]$)

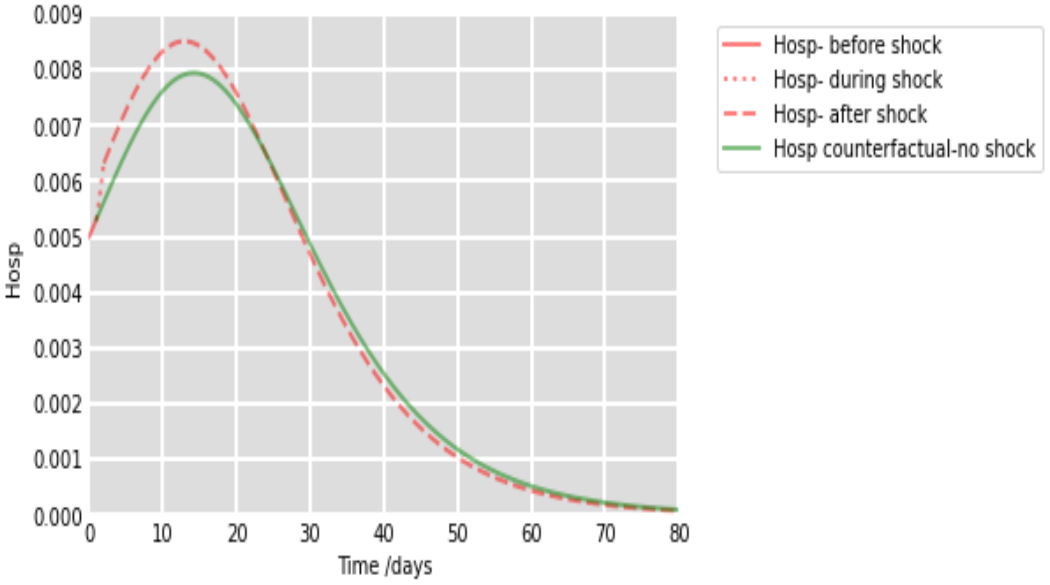

We also see in Figure 3 that the flow of new hospitalizations is larger than that of the

counterfactual till around $t = 25$ and then is slightly lower. This property strongly depends on the timing of the shock, as detailed in the following proposition.

Lemma 6. *After the mobility shock, the difference between the flow associated with the shocked trajectory and that of the counterfactual decreases if the shock occurred before the epidemic peak. Otherwise, the difference may temporarily continue to increase after the shock.*

Proof. See the Appendix. □

This is illustrated with a simulation. Figure 4 represents the two trajectories for a shock occurring after the epidemic peak. The gap decreases monotonously.

Figure 4: Inflow of new hospitalizations ($H_{osp}(t)$) along the shocked trajectory ($k_1 = 0.8$ for all $t \in [0, 50] \setminus [30, 31]$ and $k_1 = 0.7$ for $t \in [30, 31]$) and the counterfactual case ($k_1 = 0.8$ for all $t \in [0, 50]$)

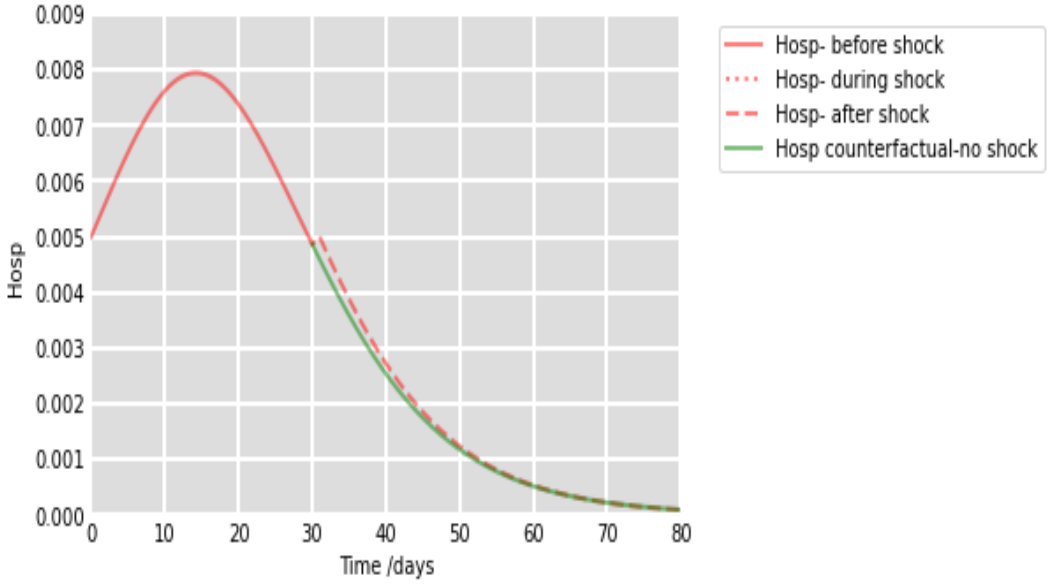

If the shock occurs before the epidemic peak, we notice that the gap increases after the time interval during which the shock occurred. It is therefore possible that the flow of new hospitalizations is ultimately lower than in the counterfactual. Nevertheless, we show that the total number of new hospitalizations is higher over the whole shocked trajectory.

Lemma 7. *The number of individuals who did not become infected during the epidemic is lower in the positive mobility shock case than in the counterfactual case.*

Proof. See the Appendix. □

We now evaluate the effect of an exogenous shock on new hospitalizations. We start with the following result:

Lemma 8. *An increase in new hospitalizations immediately reduces mobility.*

Proof. See the Appendix. □

This result is illustrated by simulations of the effect of a temporary change in parameter c. Figure 5 represents the evolution of mobility following a decrease of c from 0.4 to 0.2 during the time interval [1,2]. The new trajectory (gray curve) passes under the trajectory without shock (green curve).

Figure 5: Mobility ($m(t)$) along the shocked trajectory ($c = 0.4$ for all $t \in [0, 50] \setminus [1, 2]$ and $c = 0.2$ for $t \in [1, 2]$) and the counterfactual case ($c = 0.4$ for all $t \in [0, 50]$)

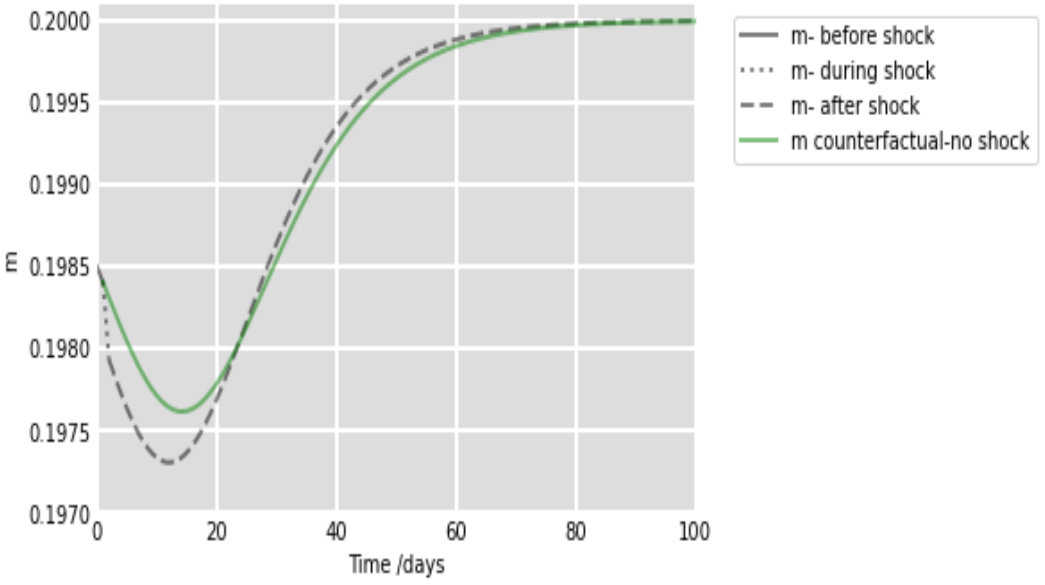

Again, the mobility of the path with mobility shock eventually rises above the counterfactual path. This does not happen if the shock occurs after the epidemic peak. For example, in Figure 6, the shock to c occurs over the time interval [30-31].

Figure 6: Mobility ($m(t)$) along the shocked trajectory ($c = 0.4$ for all $t \in [0, 50] \setminus [30, 31]$ and $c = 0.2$ for $t \in [30, 31]$) and the counterfactual case ($c = 0.4$ for all $t \in [0, 50]$)

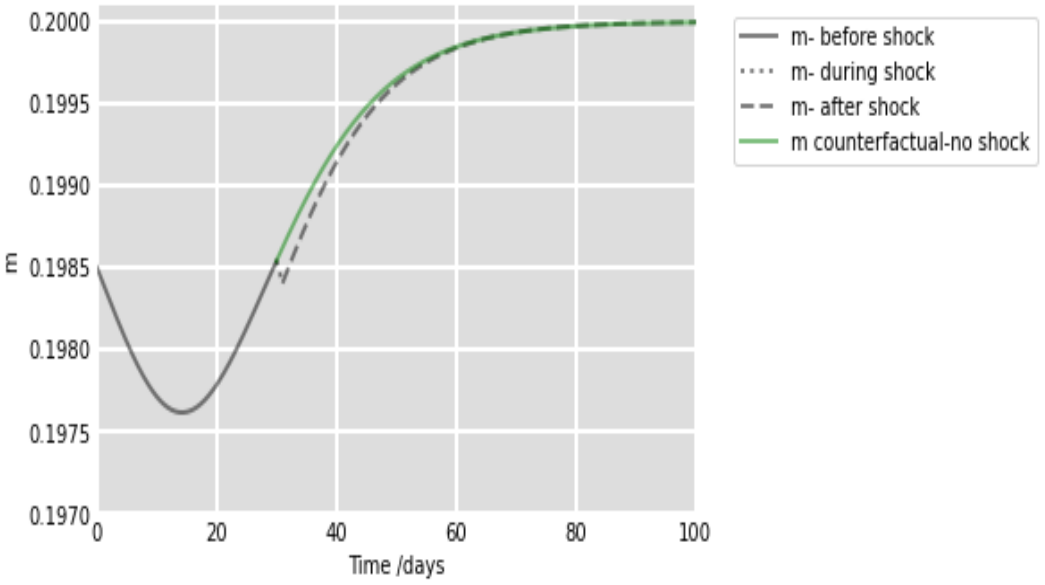

3 Empirical Evidence from French Regions

We analyse the dynamic interactions between the COVID-19 epidemic and mobility. We follow d'Albis et al. (2021) and estimate a panel vector autoregressive (VAR) model using weekly data on hospital admissions due to COVID-19 in 96 French administrative regions (*départements*) from March 23, 2020 to March 21, 2021 (52 weeks). The data are official and publicly available at `www.data.gouv.fr`. The hospitalizations due to COVID-19 were consistently measured over the period and are thus more reliable than the series that report the number of infections, as the latter highly depend on the availability of tests and on the population's willingness to get tested. Daily data are available since March 19, 2020, but we choose to use the weekly frequency in order to avoid a seasonal effect induced by lower reporting during weekends. We limit the time window to March 2021 to avoid the effects of the vaccination campaign that started in France in early 2021. Mobility data come from the Facebook Data for Good program's data sets. People who use Facebook on a mobile device have the option of providing their precise location. The program produces various aggregated indicators using these data, including a quantification of how much people move around by counting the number of level-16 Bing tiles (which are approximately 600 meters by 600 meters in area at the equator) they are

seen in within a day. The data are available at the administrative regions level we considered and are given as a deviation with respect to the observed mobility in February 2020.

The model is written as:

$$Y_{it} = \sum_{s=1}^{p} \Phi_s Y_{it-s} + \alpha_i + \beta_i.t + \eta_t + u_{it} \;\; i = 1, ..., N \text{ and } t = 1, ..., T \tag{20}$$

where $Y_{it} = (h_{it}, m_{it})'$ is a 2-dimensional vector of endogenous variables including the logarithm of 1 plus the pandemic-induced hospitalizations (h_{it}) and the mobility (m_{it}); Φ_s are fixed (2×2) matrices of coefficients $\alpha_i = (\alpha_i^1, \alpha_i^2)'$ is a vector of regional fixed-effects; $\beta_i.t = (\beta_i^1, \beta_i^2)'.t$ represent region specific-time (linear) trend, $\eta_t = (\eta_t^1, \eta_t^2)$ is a vector of common (national) time (week)-specific effect (such as national lockdown); $u_{it} = (u_{it}^1, u_{it}^2)'$ is a 2-dimensional vector of errors with the assumption that $E(u_{it}) = 0$ and $E(u_{it}u_{i\tau}') = \Sigma.1_{t=\tau}$ for all t and τ.

The results of preliminary diagnostics (panel unit root tests) reject the null hypothesis of unit root for the de-trended variables (with a region-specific linear trend).Therefore, in the VAR system, we use variables in level (or log level) and control for region heterogeneity (by introducing region-specific effects and region-specific time trends) and cross-region interdependence (by introducing week-specific effects). As noted in the Introduction, the latter fixed effects are particularly important as they control for any national-level determinant, such as national policies in response to the Covid-19 epidemic. Following d'Albis et al. (2021), the model is estimated by the bias-corrected fixed-effect estimator developed by Hahn and Kuersteiner (2002). We set the lag length p to 3 based on the Bayesian information criterion (BIC) and the Hannan-Quinn information criterion (HQC). Considering a lag length higher than 3 does not change our findings.

After having estimated the VAR model, to compute the dynamic responses between variables, we identify the structural shocks ω_{it} using the Cholesky decomposition so that $\omega_{it} = Bu_{it}$, where B is the unique lower-triangular Cholesky factor of Σ.

This decomposition relies on the assumption that variables ordered first in the VAR can impact the other variables contemporaneously, whereas variables ordered later can impact those ordered first only with lags. The Cholesky identification assumptions are about the

contemporary impacts of the examined shocks, and no restriction is placed upon the variables for periods after one week. We rely on the results derived from our theoretical model (Lemma 3) to impose that a shock on the pandemic-induced hospitalisations can impact mobility in the same period (week) whereas a shock on mobility can impact hospitalisations only with lags (after one week). We, therefore, order hospitalizations first and mobility second. Nevertheless, we note that the alternative ordering does not qualitatively modify the results (See the Appendix).

The dynamic responses are displayed in Figure 7, with the dashed lines being 90% confidence intervals. Hospitalisations respond positively to mobility, and this response is statistically significant 3 weeks after the shock onwards. In terms of magnitude, a 10% increase in mobility index (with respect to its sample average, which is -0.14) induces 28 new hospitalizations one week after the shock and 84 new hospitalisations at the peak (i.e. 3 weeks after the shock). During the March 2020's lockdown, mobility index dropped by around 0.6 which is 42 times larger than the shock we consider; more than 3500 (42*84) hospitalisations may then have been avoided thanks to a fall in mobility, about 50% of average weekly number of new hospitalisations over the considered period. Conversely, one week after a rise in hospitalisations, mobility falls in a statistically significant manner. However, the magnitude of the mobility response is very small since a 10% increase in new hospitalisations induces a reduction of the mobility index (at its sample mean) of 0.24% at the peak (i.e. 2 weeks after the shock). In other words, we find little evidence for a substantial behavioural reaction of the population to higher COVID-19 cases.

Our empirical results are quite robust to the addition of potentially relevant additional variables. We first included the number of reported cases of infection. This information, ahead of hospitalizations, may potentially modify the mobility in the population. We obtained that our findings were barely modified (See the Appendix for details). Second, we took into account that climatic conditions may matter for the transmission of the SARS-CoV-2 (Briz-Redón and Serrano-Aroca (2020), Marazziti et al. (2021), d'Albis et al. (2021)). We check the robustness of our findings by controlling for local temperature and humidity. Following d'Albis et al. (2021), we include in our model the IPTCC index, which is a function of absolute humidity

Figure 7: Dynamic responses between mobility and hospitalisations

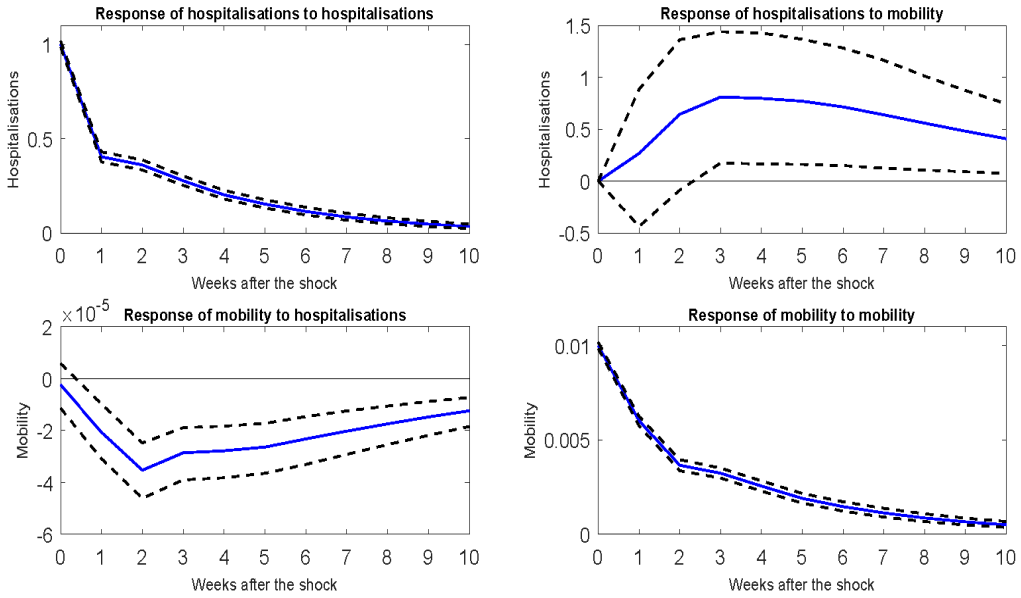

Notes: The solid line gives the estimated impulse responses. Dashed lines give the 90% confidence intervals generated by Monte Carlo with 5,000 repetitions. The size of shock on hospitalizations is set to one percent increase; the size of mobility shock is set to 0.01 unit increase in the Facebook mobility index. The response of hospitalizations is in percent change; the response of mobility is in unit increase.

(AH), relative humidity (RH), and temperature (T), and the formula can be written as follows:

$$IPTCC = 100e^{-0.5\left[\left[\frac{(T-7.5)^2}{196}+\frac{(RH-75)^2}{625}+\frac{(AH-6)^2}{2.89}\right]\right.}. \quad (21)$$

The IPTCC is thus maximal when the temperature reaches 7.5°C and the relative humidity 75%. The meteorological data came from the 63 Météo-France stations, which are homogeneously distributed over mainland France in order to represent the diversity of the country's climate. However, data are only provided for 54 administrative regions, which means a small sample. Since climatic conditions are exogenous with respect to hospitalisations and mobility, we rely on the following panel VARX structure (VAR model with exogenous variables):

$$Y_{it} = \sum_{s=1}^{p} \Phi_s Y_{it-s} + \sum_{s=1}^{p} \gamma_s cl_{it-s} + \alpha_i + \beta_i.t + \eta_t + u_{it} \;\; i = 1, ..., N \text{ and } t = 1, ..., T \quad (22)$$

where cl_{it} represents climate conditions proxied by the IPTCC. The dynamic responses from this extended VAR system are reported in Figure 8. We observe that the responses are qualitatively

the same.

Figure 8: Dynamic responses between mobility and hospitalisations, controlling for climate conditions

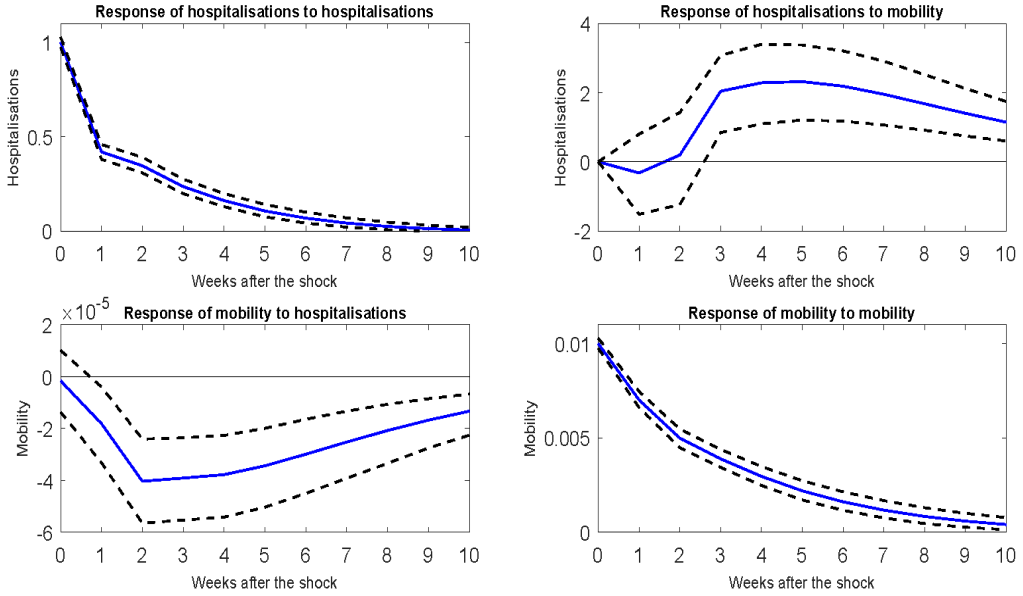

Notes: The solid line gives the estimated impulse responses. Dashed lines give the 90% confidence intervals generated by Monte Carlo with 5,000 repetitions. The size of shock on hospitalizations is set to one percent increase; the size of mobility shock is set to 0.01 unit increase in the Facebook mobility index. The response of hospitalizations is in percent change; the response of mobility is in unit increase.

4 Conclusion

In this paper we have shown, theoretically and empirically, that mobility and COVID-19 infection rates are jointly determined, with some lag. However, in contrast with a large, mainly US-focused literature, we find that voluntary social distancing cannot explain the large mobility reductions observed in France. This stark finding suggests that modelling of a contagious disease such as COVID-19 needs to incorporate feedback effects moderated by context-specific factors. What are these moderating factors? While economists often feel uneasy about attributing a role to culture in explaining variations in cross-country outcomes, citizens' values and beliefs are obvious candidates. It is possible that, in France, restraints on individual behaviours are strongly shaped by government policies. This is a topic of crucial health and economic importance that ought to be explored in further research. This work reveals the value of incorporating

mobility behaviors into epidemic models. We have done this in a relatively simple way, by making the rate of infection dependent on mobility. It would certainly be useful to extend this work by studying other types of relationships and other functional forms.

References

Allen, Douglas W. (2021) 'Covid-19 Lockdown Cost/Benefits: A Critical Assessment of the Literature', *International Journal of the Economics of Business*, forthcoming.

Arino, Julien, Brauer, Fred, van den Driessche, Pauline, Watmough, James, and Wu, Jianhong (2006) 'Simple Models for Containment of a Pandemic', *Journal of the Royal Society Interface*, Vol. 3, pp. 453–457.

Aubert, Cécile and Augeraud-Véron, Emmanuelle (2021) 'The Relative Power of Individual Distancing Efforts and Public Policies to Curb the COVID-19 Epidemics', *PLoS One*, Vol. 16, p. e0250764.

Augeraud-Véron, Emmanuelle (2020) 'Lifting the COVID-19 Lockdown: Different Scenarios for France', *Mathematical Modelling of Natural Phenomena*, Vol. 15, p. 40.

Bricongne, Jean-Charles and Meunier, Baptiste (2021) 'Social and Economic Impact of COVID-19', VOXEU, available at `https://voxeu.org/article/best-policies-fight-pandemics-five-lessons-literature-so-far`.

Briz-Redón, Álvaro and Serrano-Aroca, Ángel (2020) 'The Effect of Climate on the Spread of the COVID-19 Pandemic: A Review of Findings, and Statistical and Modelling Techniques', *Progress in Physical Geography: Earth and Environment*, Vol. 44, pp. 591–604.

Brodeur, Abel, Gray, David, Islam, Anik, and Bhuiyan, Suraiya (2021) 'A Literature Review of the Economics of COVID-19', *Journal of Economic Surveys*, Vol. 35, pp. 1007–1044.

Carnehl, Christoph, Fukuda, Satoshi, and Kos, Nenad (2023) 'Epidemics with Behavior', *Journal of Economic Theory*, Vol. 207.

Caselli, Francesca, Grigoli, Francesco, and Sandri, Damiano (2021) 'Protecting Lives and Livelihoods with Early and Tight Lockdowns', *The BE Journal of Macroeconomics*, forthcoming.

Chernozhukov, Victor, Kasahara, Hiroyuki, and Schrimpf, Paul (2021) 'Causal Impact of Masks, Policies, Behavior on Early covid-19 Pandemic in the US', *Journal of Econometrics*, Vol. 220, pp. 23–62.

Citron, Daniel T, Guerra, Carlos A, Dolgert, Andrew J, Wu, Sean L, Henry, John M, Smith, David L et al. (2021) 'Comparing Metapopulation Dynamics of Infectious Diseases Under Different Models of Human Movement', *Proceedings of the National Academy of Sciences*, Vol. 118.

Van den Driessche, Pauline and Watmough, James (2002) 'Reproduction Numbers and Sub-threshold Endemic Equilibria for Compartmental Models of Disease Transmission', *Mathematical biosciences*, Vol. 180, pp. 29–48.

d'Albis, Hippolyte and Augeraud-Véron, Emmanuelle (2021) 'Optimal Prevention and Elimination of Infectious Diseases', *Journal of Mathematical Economics*, Vol. 93, p. 102487.

d'Albis, Hippolyte, Coulibaly, Dramane, Roumagnac, Alix, de Carvalho Filho, Eurico, and Bertrand, Raphaël (2021) 'Quantification of the Effects of Climatic Conditions on French Hospital Admissions and Deaths Induced by SARS-CoV-2', *Scientific reports*, Vol. 11, pp. 1–7.

Eichenbaum, Martin S, Rebelo, Sergio, and Trabandt, Mathias (2021) 'The Macroeconomics of Epidemics', *The Review of Financial Studies*, Vol. 34, pp. 5149–5187.

Escandón, Kevin, Rasmussen, Angela L, Bogoch, Isaac I, Murray, Eleanor J, Escandón, Karina, Popescu, Saskia V, and Kindrachuk, Jason (2021) 'COVID-19 False Dichotomies and a Comprehensive Review of the Evidence Regarding Public Health, COVID-19 Symptomatology, SARS-CoV-2 Transmission, Mask wearing, and Reinfection', *BMC Infectious Diseases*, Vol. 21, pp. 1–47.

Fabbri, Giorgio, Federico, Salvatore, Fiaschi, Davide, and Gozzi, Fausto (2023) 'Mobility decisions, economic dynamics and epidemic', *Economic Theory*, URL: https://doi.org/10.1007/s00199-023-01485-1.

Fernández-Villaverde, Jesús and Jones, Charles I (2020) 'Macroeconomic Outcomes and COVID-19: a Progress Report', NBER Working Paper, No 28004.

Galeazzi, Alessandro, Cinelli, Matteo, Bonaccorsi, Giovanni, Pierri, Francesco, Schmidt, Ana Lucia, Scala, Antonio, Pammolli, Fabio, and Quattrociocchi, Walter (2021) 'Human Mobility in Response to COVID-19 in France, Italy and UK', *Scientific Reports*, Vol. 11, pp. 1–10.

Goenka, Aditia, Liu, Lin, and Nguyen, Manh-Hung (2022) 'Modelling optimal lockdowns with waning immunity', *Economic Theory*, URL: https://doi.org/10.1007/s00199-022-01468-8.

Goolsbee, Austan and Syverson, Chad (2021) 'Fear, Lockdown, and Diversion: Comparing Drivers of Pandemic Economic Decline 2020', *Journal of Public Economics*, Vol. 193, pp. 1–8.

Hahn, Jinyong and Kuersteiner, Guido (2002) 'Asymptotically Unbiased Inference for a Dynamic Panel Model with Fixed Effects When Both N and T Are Large', *Econometrica*, Vol. 70, pp. 1639–1657.

Hritonenko, Natali and Yatsenko, Yuri (2022) 'Analysis of optimal lockdown in integral economic–epidemic model', *Economic Theory*, URL: https://doi.org/10.1007/s00199-022-01469-7.

Joffe, Ari R (2021) 'COVID-19: Rethinking the Lockdown Groupthink', *Frontiers in Public Health*, Vol. 9, pp. 1–25.

La Torre, Davide, Liuzzi, Danilo, Maggistro, Rosario, and Marsiglio, Simone (2022) 'Mobility Choices and Strategic Interactions in a Two-Group Macroeconomic–Epidemiological Model', *Dynamic Games and Applications*, Vol. 12, pp. 110–132.

Levy Yeyati, Eduardo and Filippi, Federico (2021) 'Social and Economic Impact of COVID-19', Brookings Global Working Paper, No. 158.

Liu, Zhihua, Magal, Pierre, Seydi, Ousmane, and Webb, Glenn (2020a) 'Predicting the Cumulative Number of Cases for the COVID-19 Epidemic in China From Early Data', *Mathematical Biosciences and Engineering*, Vol. 17, pp. 3040–3051.

——— (2020b) 'Understanding Unreported Cases in the COVID-19 Epidemic Outbreak in Wuhan, China, and the Importance of Major Public Health Interventions', *Biology*, Vol. 9, p. 50.

Makris, Miltiadis (2021) 'Covid and social distancing with a heterogenous population', *Economic Theory*, Vol. To appear.

Marazziti, Donatella, Cianconi, Paolo, Mucci, Federico, Foresi, Lara, Chiarantini, Ilaria, and Della Vecchia, Alessandra (2021) 'Climate Change, Environment Pollution, COVID-19 Pandemic and Mental Health', *Science of The Total Environment*, Vol. 773, p. 1451182.

Milani, Fabio (2021) 'COVID-19 Outbreak, Social Response, and Early Economic Effects: A Global VAR Analysis of Cross-Country Interdependencies', *Journal of Population Economics*, Vol. 34, pp. 223–252.

Philipson, Tomas (2000) 'Economic Epidemiology and Infectious Diseases', Vol. 1: Elsevier, pp. 1761–1799.

Pullano, Giulia, Valdano, Eugenio, Scarpa, Nicola, Rubrichi, Stefania, and Colizza, Vittoria (2020) 'Evaluating the Effect of Demographic Factors, Socioeconomic Factors, and Risk Aversion on Mobility during the COVID-19 Epidemic in France Under Lockdown: A Population-Based Study', *The Lancet Digital Health*, Vol. 2, pp. e638–e649.

Tikhonov, Nikolaï (1952) 'Systems of Differential Equations Containing a Small Parameter Multiplying the Derivative', *Mathematical Sbornik*, Vol. 31, pp. 575–586.

5 Appendix I: Proofs of the Lemma

Proof of Lemma 1. Let us first note that since $P'(t) = -\gamma H(t)$, we have $P(t) \leq P_0$. Moreover, integrating the differential equation gives:

$$P_0 - P(t) = \gamma \int_0^t H(u)\, du. \tag{23}$$

We therefore observe that $\gamma \int_0^t H(u)\, du \leq P_0$, which implies that $\int_0^\infty H(u)\, du$ is finite and consequently $\lim_{t\to+\infty} H(t) = 0$. This also implies that $\lim_{t\to+\infty} A(t) = 0$ and $\lim_{t\to+\infty} R(t) = 0$. Furthermore, since $S'(t) < 0$, $S(t)$ decreases to $\lim_{t\to\infty} S(t) = S_\infty$. It remains to be proved that $S_\infty > 0$. To do so, we first notice that $\tau(m) < \xi$. Then, we integrate equation (5) and obtain that:

$$R(t) = \eta_1 \int_0^t A(u)\, du + \eta_2 \int_0^t H(u)\, du. \tag{24}$$

Thus, $\eta_2 \int_0^t H(u)\, du \leq 1$ and we then deduce from equation (2) that $S(t) \geq e^{\frac{\xi}{\eta_2}} > 0$. □

Proof of Lemma 2. According to Van den Driessche and Watmough (2002), the reproduction number is the spectral radius of matrix FV^{-1}, where:

$$V = \begin{bmatrix} \eta_1 + \nu & 0 \\ 0 & \eta_2 + \gamma \end{bmatrix} \text{ and } F = \tau(\overline{m})\, S_\infty \begin{bmatrix} 1 & 0 \\ 0 & 0 \end{bmatrix}. \tag{25}$$

Then, simple algebra using (25) gives (10). □

Proof of Lemma 3. In the following, notation $\dot{x}$ stands for $dx(z)/dz$. At fast time z, System $\mathcal{P}$ is a regular perturbation of the following unperturbed system:

$$\dot{S}(z) = 0, \tag{26}$$

$$\dot{A}(z) = 0, \tag{27}$$

$$\dot{H}(z) = 0, \tag{28}$$

$$\dot{m}(z) = \lambda(1 - k_1 - k_2 \nu A(z) - m(z)). \tag{29}$$

At fast time, the dynamics variables are constant while m varies quickly and is approximated

by the solution of the boundary layer:

$$\dot{m}(z) = \lambda(1 - k_1 - k_2\nu A(z) - m(z)). \tag{30}$$

The slow manifold, defined as $\mathcal{L} = \{(S, A, H, R, m), m = 1 - k_1 - k_2\nu A\}$, is attractive, and thus, Tikhonov (1952)'s Theorem can be applied. According to this Theorem, letting $(S_0, A_0, H_0, 0, m_0)$ be an initial condition, the solution of system $\mathcal{P}$ quickly converges to the neighborhood of the slow manifold, where the slow motion takes place. The slow motion is then given by (13)-(16). □

Proof of Lemma 4. By dividing (14) by (13), one has:

$$\frac{dA}{dS} = -1 + \frac{\nu + \eta_1}{\tau(1 - k_1 - k_2\nu A)S}, \tag{31}$$

and thus:

$$\frac{dH_{osp}}{dS} = -\nu + \frac{(\nu + \eta_1)\nu}{\tau(1 - k_1 - k_2 H_{osp})S}. \tag{32}$$

Note that $m > 0$ implies $1 - k_1 - k_2 H_{osp}$. Then, using (9), can rewrite (32) as follows:

$$\frac{dH_{osp}}{dS} = -\nu + \frac{(\nu + \eta_1)\nu}{\xi\frac{(1-k_1-k_2H_{osp})}{c+(1-k_1-k_2H_{osp})}S}. \tag{33}$$

Thus:

$$\frac{dH_{osp}}{dS} \geq 0 \Longleftrightarrow S \leq \frac{(\nu + \eta_1)}{\xi}\left(\frac{c}{1 - k_1 - k_2 H_{osp}} + 1\right), \tag{34}$$

where the RHS is increasing and convex in H_{osp}. Consequently, one has for a set of initial conditions:

$$\left.\frac{dH_{osp}}{dS}\right|_{S=S_0, H_{osp}=\nu A_0} \geq 0 \Longleftrightarrow S_0 \leq \frac{(\nu + \eta_1)}{\xi}\left(\frac{c}{1 - k_1 - k_2\nu A_0} + 1\right). \square \tag{35}$$

Proof of Lemma 5. Let us denote $[t_0, t_1]$, with $t_0 < t_1$, the interval during which the shock happens; during that time we denote it k_1^{shock}. Moreover, we denote by $H_{osp}(t)$ and $S(t)$ the trajectories with the shock, and by $H_{osp}^c(t)$ and $S^c(t)$ the counterfactual trajectory. The proof

proceeds in two steps. We first show the positivity of $H_{osp}(t) > H^c_{osp}(t)$ for $t \in [t_0, t_1]$ is proved, then we prove that $H_{osp}(t) - H^c_{osp}(t)$ is an increasing function of time during the shock. With (32), let us compute the following:

$$\frac{d}{dk_1}\left(\frac{dH_{osp}}{dS}\right) = \frac{(\nu+\eta_1)\nu}{\xi S}\frac{c}{(1-k_1-k_2H_{osp})^2} > 0. \tag{36}$$

Step 1: Proof of $H_{osp}(t) > H^c_{osp}(t)$ for $t \in [t_0, t_1]$. First notice that during the shock, trajectories $t \mapsto (S(t), H_{osp}(t))$ and $t \mapsto \left(S^c(t), H^c_{osp}(t)\right)$ do not intersect. Given (36) we have that $k_1^{shock} < k_1$ implies that $\frac{dH_{osp}}{dS} < \frac{dH^c_{osp}}{dS^c}$ at any point of intersection. Thus, there exists ω such that: $H_{osp}(S(t_0) - w) > H^c_{osp}(S(t_0) - w)$, for $0 < w < \omega$. Let us remark that in the previous expression, as we are considering phase plane trajectory, H_{osp} and H^c_{osp} are seen as function of the number of susceptible (and not time). If the two curves would intersect, there would exist some $\widehat{S}$, such that $H_{osp}\left(\widehat{S}\right) = H^c_{osp}\left(\widehat{S}\right)$, with $\widehat{S} = \{S \in (S(t_0) - \omega, S(t_0), H_{osp}\left(\widehat{S}\right) = H^c_{osp}\left(\widehat{S}\right)\}$. Then $\frac{dH_{osp}}{dS}\left(\widehat{S}\right) > \frac{dH^c_{osp}}{dS}\left(\widehat{S}\right)$, which leads to a contradiction. This first part of the proof is an adaptation of the Proposition 5 of Carnehl et al. (2023).

Step 2a: Proof of $H_{osp}(t) - H^c_{osp}(t)$ being an increasing function of t if the shock happens before the epidemic peak. During the shock, we have $\frac{d}{dk_1}\left(\frac{dS}{dt}\right) > 0$, and thus $\frac{dS}{dt} < \frac{dS^c}{dt}$. As $\frac{dS^c}{dt} < 0$, the following inequality holds:

$$\frac{\frac{dS}{dt}}{\frac{dS^c}{dt}} > 1. \tag{37}$$

Moreover, according to (36), we have: $\frac{dH_{osp}}{dS} < \frac{dH^c_{osp}}{dS^c}$, and thus:

$$\frac{dH_{osp}/dt}{dS/dt} < \frac{dH^c_{osp}/dt}{dS^c/dt}. \tag{38}$$

It thus imply, as $dS/dt < 0$ and $dH^c_{osp}/dt > 0$ before the epidemic peak, that:

$$\frac{dH_{osp}/dt}{dH^c_{osp}/dt} > \frac{dS/dt}{dS^c/dt} > 1. \tag{39}$$

As a consequence, $H_{osp}(t) - H^c_{osp}(t)$ is an increasing function of t for $t \in [t_0, t_1]$.

Step 2b: Proof of $H_{osp}(t) - H^c_{osp}(t)$ being an increasing function of t if the shock happens after the epidemic peak. The previous step remains valid up to (38). However, as after the epidemic peak $dH^c_{osp}/dt < 0$, then the same reasoning does not permit to conclude, as it leads to the following inequalities:

$$\frac{dS/dt}{dS^c/dt} > 1 \text{ and } \frac{dH_{osp}/dt}{dH^c_{osp}/dt} < \frac{dS/dt}{dS^c/dt}. \tag{40}$$

Thus we directly consider $\frac{d}{dk_1}\left(\frac{dH}{dt}\right) < 0$, thus $\frac{dH}{dt} > \frac{dH^c}{dt}$ during the shock. Notice that the same proof could have been done in step 2, but we wanted to highlight a key difference between what happens during the epidemiological peak and what happens after. □

Proof of Lemma 6. The proof has to be decomposed according the timing of the shock. We first prove that if t_1 is larger than the date at which the epidemic peak occurs in the shocked-trajectory, then $H_{osp}(t) - H^c_{osp}(t)$ is a decreasing as a function of t. Then, we show that if t_1 is larger than the date at which the epidemic peak occurs, there may exist $t_2 > t_1$, such that $H_{osp}(t) - H^c_{osp}(t)$ is increasing on $[t_1, t_2]$.

Before detailing the proof, we just notice that phase space trajectories with initial conditions $(S(t_1), H_{osp}(t_1))$ and $\left(S^c(t_1), H^c_{osp}(t_1)\right)$ do not intersect as the shocked trajectory and the counterfactual trajectory are now given by the same dynamic system. As a consequence, it can be noticed that $S(\infty) < S^c(\infty)$. Moreover, from the proof of Lemma 5, we know that $S(t_1) < S^c(t_1)$ and $H_{osp}(t_1) > H^c_{osp}(t_1)$. Thus, the shocked trajectory may have reach the epidemic peak whereas the counterfactual model hasn't yet.

Step 1: Proof in the case t_1 is larger than the date at which the epidemic peak occurs in the shocked-trajectory. Notice first that if the shocked trajectory has reached its epidemiological peak, i.e. if $\frac{dH_{osp}(t)}{dt} < 0$, whereas the counterfactual hasn't yet, i.e. if $\frac{dH^c_{osp}(t)}{dt} > 0$, it is straightforward that $H_{osp}(t) - H^c_{osp}(t)$ is a decreasing function of t. Let us now assume that both epidemic curves have reached their epidemiological peak. The growth rate of the inflow

of newly hospitalized is:

$$\frac{H'_{osp}}{H_{osp}} = \tau\left(1 - k_1 - k_2 H_{osp}\right) S - \nu - \eta_1. \tag{41}$$

After the shock, as the phase plane trajectories do not intersect, we either have $H_{ops}(t) > H^c_{ops}(t)$ and $S(t) \leq S^c(t)$ or $H_{ops}(t) \geq H^c_{ops}(t)$ and $S(t) < S^c(t)$. It thus comes:

$$\frac{H'_{osp}}{H_{osp}} < \frac{H^{c\prime}_{osp}}{H^c_{osp}}. \tag{42}$$

As $H^{c\prime}_{osp} < 0$, then $\frac{H'_{osp}}{H^{c\prime}_{osp}} > \frac{H_{osp}}{H^c_{osp}} \geq 1$. Thus, $H'_{osp} < H^{c\prime}_{osp}$, which explains why after the peak, the inflow of new hospitalized compared to the counterfactual case is decreasing.

Step 2: Proof in the case t_1 is smaller than the timing of the epidemic peak in the shocked-trajectory. Here, we aim at showing there exists conditions under which $H'_{osp}\left(t_1^+\right) - H^{c\prime}_{osp}\left(t_1^+\right) > 0$. Notice that if we follow the same reasoning than in Step 1, the two following inequalities (that do not permit to conclude) are obtained:

$$\frac{H'_{osp}}{H^{c\prime}_{osp}} < \frac{H_{osp}}{H^c_{osp}} \text{ and } \frac{H_{osp}}{H^c_{osp}} > 1. \tag{43}$$

The larger $H_{osp}(t_1)$ compared to $H^c_{osp}(t_1)$, the greater the possibility than $1 < \frac{H'_{osp}}{H^{c\prime}_{osp}}$. This condition thus depends on the magnitude of the shock, on its duration and also on the timing of the shock. Indeed, the higher the magnitude, the smaller the duration and the earlier the shock happens compared to the epidemic peak, the more likely the situation $H'_{osp}\left(t_1^+\right) - H^{c\prime}_{osp}\left(t_1^+\right) > 0$ may occur. □

Proof of Lemma 7. Please refer to the proof of Lemma 6. □

Proof of Lemma 8. According to Tikhonov (1952)'s Theorem, $m(t)$ rapidly adjust to:

$$m(t) = 1 - k_1 - k_2 H_{osp}(t). \square \tag{44}$$

6 Appendix II: Additional Estimations

The impulse-responses provided in Figure 9 are the counterpart of those presented in Figure 7, except we modified the ordering of the variables in the Cholesky decomposition. Mobility is ordered first while hospitalizations are ordered second. We see that responses are barely modified.

Figure 9: Dynamic responses between mobility and hospitalisations, using alternative ordering

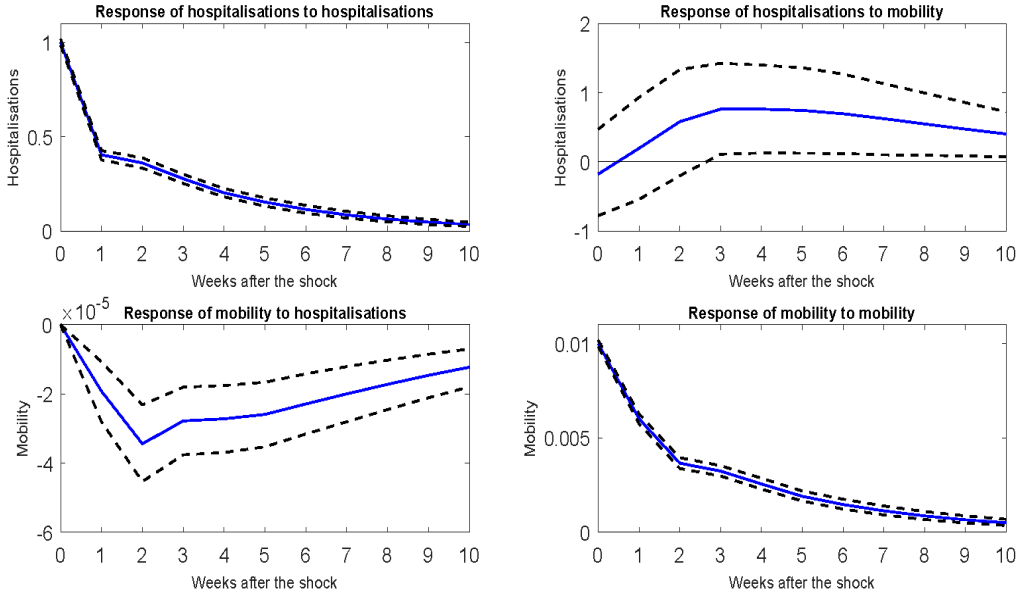

Notes: The solid line gives the estimated impulse responses. Dashed lines give the 90% confidence intervals generated by Monte Carlo with 5,000 repetitions. The size of shock on hospitalizations is set to one percent increase; the size of mobility shock is set to 0.01 unit increase in the Facebook mobility index. The response of hospitalizations is in percent change; the response of mobility is in unit increase.

Figure 10 presents the impulse-responses of an extended model that includes the weekly number of reported cases of infection. To identify shocks in this extended system, we order first cases in the Cholesky decomposition, since hospitalisations may immediately respond to cases. We see that including the number of reported cases does not alter the dynamic interaction between hospitalisations and mobility.

Figure 10: Dynamic responses between mobility, hospitalisations and cases

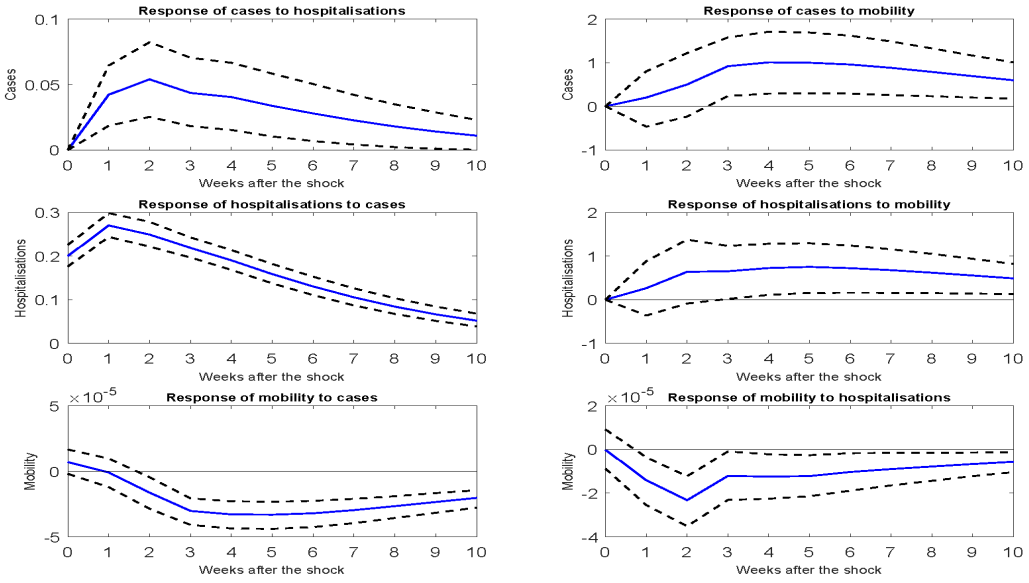

Notes: The solid line gives the estimated impulse responses. Dashed lines give the 90% confidence intervals generated by Monte Carlo with 5,000 repetitions. The size of shock on cases and hospitalizations are set to one percent increase; the size of mobility shock is set to 0.01 unit increase in the Facebook mobility index. The response of cases and hospitalizations are in percent change; the response of mobility is in unit increase.